

ISSN No. 2454-6194 | DOI: 10.51584/IJRIAS | Volume X Issue IX September 2025

# Design of Uniform Spray Nozzle and Simulation of Carrier Gas Flow Rate Distribution for FTO Thin Film Fabrication Process

HyeSuk Ri, SongHyok Han, NamChol Yu\*, GiWon Yang, GwangRyong Choe

Faculty of Electronics, Kim Chaek University of Technology, Pyongyang, Democratic People's Republic of Korea

\*Corresponding Author

DOI: https://dx.doi.org/10.51584/IJRIAS.2025.100900096

Received: 16 August 2025; Accepted: 23 August 2025; Published: 25 October 2025

#### **ABSTRACTS**

The FTO thin films were deposited on 15 cm  $\times$  15 cm glass substrates by ultrasonic spray pyrolysis and the influence of process parameters on the film properties was investigated. This paper is the first report on the design of a uniform nozzle and simulating the carrier gas flow characteristics in an ultrasonic spray pyrolysis process. The uniformity of FTO films was evaluated by surface resistivity. The structure, surface morphology and optical properties of FTO films were investigated using scanning electron microscopy, X-ray diffraction, and UV-Vis spectroscopy. The process conditions for film preparation were SnCl4 concentration of 1.34 mol, NH4F concentration of 0.08 mol, temperature of 500 °C, deposition time of 15 min, carrier gas flow rate of 3 m/s, distance between nozzle and substrate of 0.7 cm. The transmittance of the fabricated FTO films was 80%, the surface resistance showed a uniform behavior at 14-15 $\Omega$ /cm and the X-ray analysis showed a high orientation of SnO2 crystals in the 200-plane. SEM analysis showed that the crystallite size was constant.

Keywords: Nozzle; Design; FTO film; Simulation; Ultrasonic spray pyrolysis

## INTRODUCTION

Transparent conductive films have been widely used in solar cells [1] or thermal-reflective glass [2,3] optoelectronic devices [4,5] due to their high transmittance in the visible and near infrared regions and high reflectivity in the far infrared regions.

To improve the electrical conductivity and transmission properties of transparent conductive films, tin oxide is doped with In and Sb [6], F [7], Ce, Fe [8], Mn [9] Co [10], Mo [11], rare earth elements Pr [12], Nb [13], Ce [14], La [15], Pd and Nb.

Among these impurities, fluorine added from ammonium fluoride (NH4F) is the most commercially available because of its low cost and simple processing.

There are several methods for preparing transparent conductive films, such as the spray pyrolysis method [18, 19] and the chemical vapor deposition method, such as the sol-gel method [16, 17].

Many researchers have prepared FTO thin films under different process and reaction conditions and investigated the electro-optical properties.

Bogle et al. [22] used spin-coating technique to obtain FTO films, with resistivity varying from  $1.01\times103$  to  $7.3\times103\Omega$ /cm. The thin film doped with Gd in SnO2 layer was obtained by Adjimi [23], using spray pyrolysis technique, in which the resistivity decreased from  $1.94\times10-3$  to  $1.02\times10-3$ /cm when Gd was added to SnO2 at 0-3%. Banyamin et al. [24] prepared FTO films using magnetron sputtering technique and their analysis showed that the charge carrier concentration of undoped FTO films was  $5.5\times1018$ /cm3, while the charge carrier concentration in the doped case was  $1.46\times1020$ /cm3. Yadav et al. [25] prepared SnO2:F films by changing the substrate temperature using atomization technique, where the charge carrier concentration





decreased from 3.63×1018/cm3 to 0.98×1020/cm3 when oxygen vacancies decreased at high temperature. Kumar et al. [26] coated FTO films with NSP method, where the mobility increased from 15.88 m2V-1s-1 to 37.23 m2V-1s-1 with increasing solvent volume. Elangovan et al. [27] found that the maximum carrier mobility for FTO film thickness of 1.2 lm is 24.7 m2V-1s-1.

Among various deposition methods, spray pyrolysis or atmospheric pressure chemical vapor deposition have the advantage of low cost of thin film fabrication.

The reported properties of FTO films prepared using spray pyrolysis and atmospheric pressure chemical vapor deposition are shown in Table 1.

Table 1. Surface resistance, transmittance resistance, quality factor and deposition method of FTO films fabricated under different conditions.

6.5	70	7.0	_	Spray Pyrolysis	[16]	
10.0	75	4.5	16.5	Spray Pyrolysis	[17]	
4.4	80	3.3	7.64	Spray Pyrolysis	[18]	
4.0	78	2.7	1.74	c-AACVD	[19]	
18.0	70	_	_	APCVD	[20]	
23.3	78	3.7	_	APCVD	[21]	
_	75	6.9	8.5	APCVD	[22]	
40.0	88	13.0	_	Pulsed Laser	[23]	

Among these deposition methods, ultrasonic spray pyrolysis is a simple and cost-effective film deposition technique [36]. This method is a method of obtaining a target metal oxide film by spraying a metal salt solution containing the components of the film to be obtained using an ultrasonic transducer and then pyrolyzing it on a substrate heated with a carrier gas such as air [37]. The advantage of this method is that the ultrasonic nebulizer can obtain a uniform droplet of micrometer size and the initial velocity of the produced droplets is small, so that the pyrolysis reaction of the film can be more stable by controlling the carrier gas flow rate. Also, the low deposition temperature and precursor solvent used for film preparation are low cost due to the use of alcohol or distilled water [38]. Also, the low deposition temperature and precursor solvent used for film preparation are low cost due to the use of alcohol or distilled water.

In the process of thin film fabrication by ultrasonic spray pyrolysis, the design, rational structure and process parameters of spray nozzle, which are the main process parameters to achieve the uniformity of the thin film, are still poor in comprehensive analysis and consideration.

In this study, a novel spray nozzle was designed to fabricate homogeneous FTO films by ultrasonic spray pyrolysis, and based on simulation analysis of flow rate distribution in the nozzle, FTO films were prepared and compared with previous works.

#### **Experimental**

#### Ultrasonic spray pyrolysis process design

As reported in the literature, ultrasonic spray pyrolysis unit consists of spray process, nozzle feed process, heating process and exhaust process [20, 21]. Fig. 1 is a schematic diagram of an ultrasonic spray pyrolysis

ISSN No. 2454-6194 | DOI: 10.51584/IJRIAS | Volume X Issue IX September 2025



unit. The ultrasonic sprayer has a working frequency of 1.7 MHz and a power of 180 W, with six piezoelectric oscillators. The nozzle material is a stainless steel material with respect to its reactivity with the precursor solution.

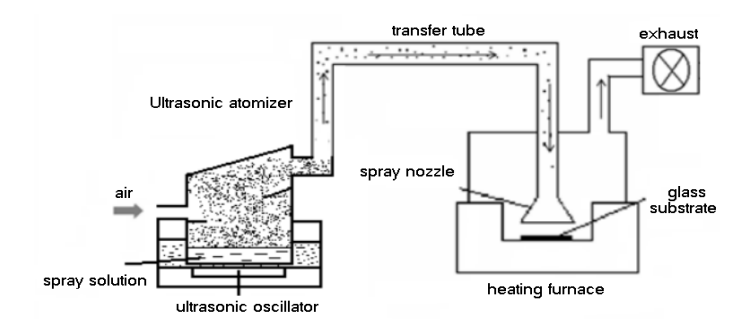


Fig. 1. Schematic diagram of ultrasonic spray pyrolysis unit.

Fig. 2 is the internal structure of the nozzle designed to provide sufficient mixing and uniform flow of the spray

The nozzle inner structure has a 2.5cm cylindrical cavity with a pipe diameter size in the pipe joint, and from this thickness it gradually narrows towards the discharge port.

The exit width is about 2mm and is mounted on the automatic feed device.

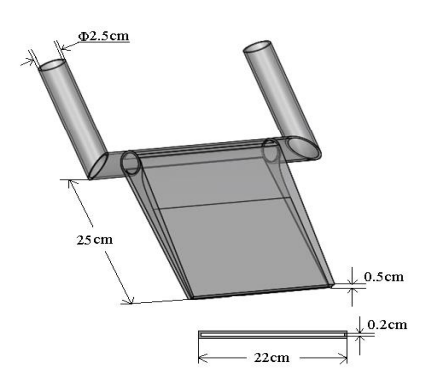


Fig. 2 nozzle design model

## **Precursor solution preparation**

The glass samples of 15×15 cm in size and 3 mm in thickness were ultrasonically cleaned with acetone, methanol and deionized water for 20 min to remove surface organics. As a precursor solution, 0.5 ml of hydrochloric acid was added dropwise to a solvent mixed with 80% distilled water and 20 ethanol, and stirred for 3min with a magnetic stirrer. Then, 1.34 mol of SnCl4•5H2O (98%) was added to the mixture, and after complete dissolution, 0.08 mol of NH4F (98%) was added and stirred again for 20 min with a magnetic stirrer. The stirred solution was filtered through a filter paper.

The prepared precursor solution was sprayed in an ultrasonic nebulizer.

The carrier gas uses air heated to 60 °C. The glass substrate temperature in the heating furnace was 500 °C and kept for 15 min to account for the heat loss during film deposition. The spray nozzle moving speed, which is set at 45° angle to the automatic feed, is 13 cm/s. The deposition time of the film was 15 min.

#### measurement analysis

XRD measurements were performed on an X-ray diffractometer (designation D8-ADVANCE, source CuKa line, scan range 0°-80°, scan rate 0.06/S). The optical transmittance of FTO films was measured by UV-Vis spectrophotometer (UV-160). The surface morphology of FTO films was measured by high-resolution SEM

ISSN No. 2454-6194 | DOI: 10.51584/IJRIAS | Volume X Issue IX September 2025

(Sign QUANTA 200). To evaluate the uniformity of the film, the organic substrate was divided into several parts and the surface resistance was measured. The surface resistance (Rsh) was obtained from the four-probe method by measuring the current (I) between two external probes, the potential difference (V) between the two internal probes and the following equation [36].

$$Rsh = 4.532(V/I)$$
 (1)

The coefficient 4.532 is applied to probes with a uniform 1 mm spacing of 1 cm  $\times$  1 cm sample size and a film thickness smaller than the spacing between probes.

#### RESULTS AND DISCUSSION

#### Simulation of the uniformity of carrier gas flow rate in spray nozzle

Fig. 3 shows the simulation results with FLUENT 6.3 for the flow rate distribution when the airflow rate of the carrier gas in the nozzle is varied from 3 to 6 m/s. The boundary condition is the density of the spray solution 1.293 kg/m3, the spray particle diameter is 1.94357 m, and the flow of carrier gas is turbulent flow mode. As shown in the figure, the larger the carrier gas flow rate, the smaller the interval with uniform flow rate gradually becomes. The reason is thought to be that the flow rate inside the nozzle increases with increasing carrier gas velocity, thereby creating pressure due to carrier gas flow inside the nozzle. When the carrier gas flow rate is less than 3m/s, the pressure inside the nozzle decreases and the uniform velocity distribution region increases, but due to the close proximity of the heated substrate and the low carrier gas flow rate, the tin oxide crystals are produced inside and outside the nozzle than the substrate. This leads to a decrease in the deposition efficiency of the film on the substrate. Of course, when looking at the nozzle and substrate after FTO film deposition, it can be seen that white crystals are deposited, which is seen as SnO2 crystals. Hence, the flow rate of air carrier gas in the spray nozzle was set to 3 m/s.

Fig.4 shows the results of the FLUENT simulations analyzed at a flow rate of 3m/s of air carrier gas. As shown in the simulation figure, the uniform velocity distribution is 17cm. Since the glass substrate is 15cm in size and the uniform velocity distribution is 17cm, this region is acceptable when the FTO film is deposited with the designed spray nozzle.

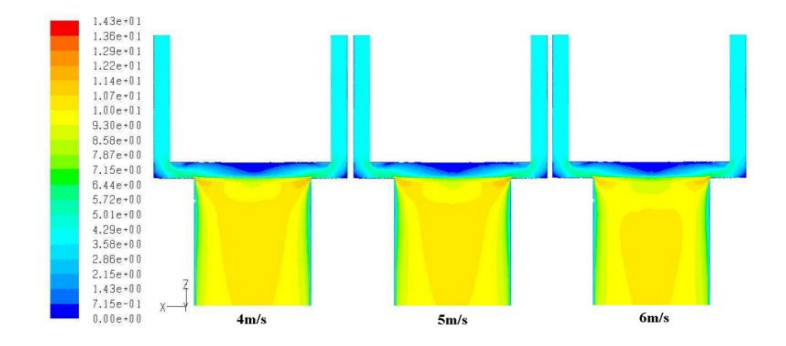


Fig. 3 Modeling of the distribution of carrier gas flow at different velocities

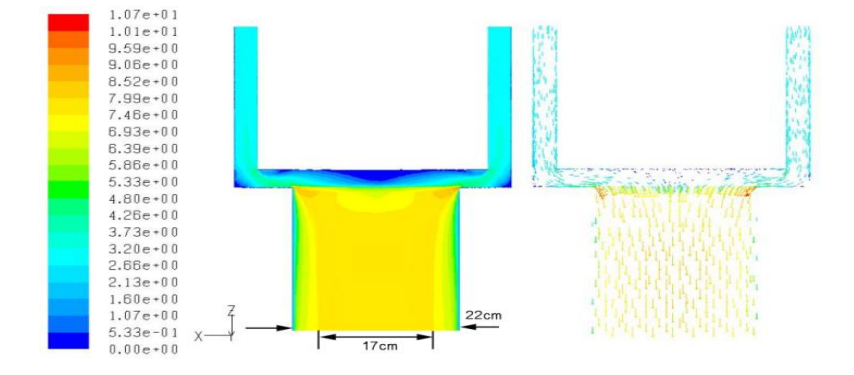


Fig. 4 Simulation results of FLUENT analysis at a flow rate of 3 m/s of air carrier gas



To verify the accuracy of the results analyzed above, we are carried out the basic experiments for FTO thin film preparation to evaluate the homogeneity of the films by surface resistivity measurements. Our basic experiments for the film homogeneity evaluation were performed by ultrasonic spray pyrolysis using the precursor solution and the experimental method described previously. Figure 5 shows the measured surface resistance values of the FTO film and several split points fabricated.

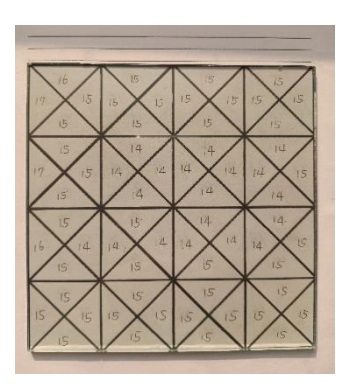


Fig.5 Surface resistance values measured on fabricated FTO films and several indexing points.

As can be seen, the surface resistance of the fabricated transparent conductive film is  $14-15\Omega/\text{cm}^2$  and only  $17\Omega/\text{cm}^2$  in one edge. This is expected because the film deposition efficiency was reduced due to heat loss at the edge of the organic substrate. The above results were also confirmed by SEM and X-ray diffraction analysis showing the microstructure and crystal morphology of the films.

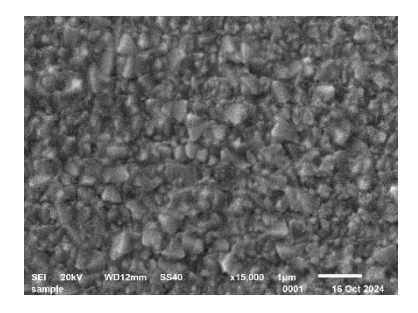


Fig. 6 SEM images of FTO thin films

As shown in Fig. 6, the grains with a clear shape and shape are uniformly distributed throughout the whole area. This is expected to contribute to the uniformity of the nozzle, although the crystal size produced during the basic experiments is constant and the surface resistance values are larger than those reported in previous studies. In addition, the XRD results of Fig. 7 showed significant crystallinity on the 200, 211, 110 and 310 planes, as reported in the literature [39]. The high intensity of the 200-plane diffraction is likely to be dominated by the crystal growth of the FTO film in the 200-plane direction due to the fluoride impurity effect.

This behavior is consistent with the data reported in the literature.

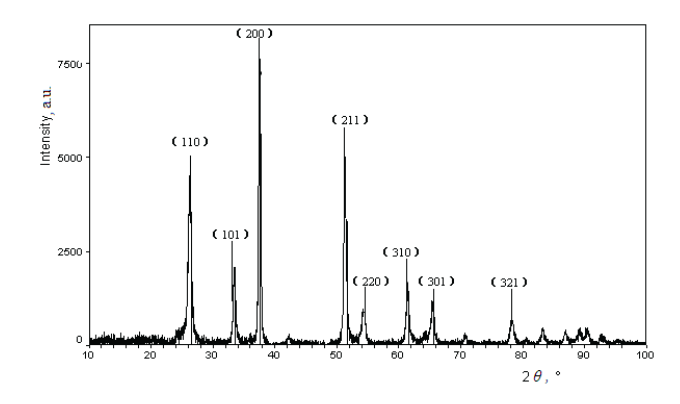


Fig. 7 X-ray diffraction data of fabricated FTO thin films





Therefore, it is thought that the designed spray nozzle is effective for deposition of uniform FTO film and the obtained film also has good characteristics as FTO film.

#### Effect of carrier gas flow rate

Based on the simulation results of the flow rate of carrier gas, a characterization of the flow rate of carrier gas was carried out. At that time, surface resistance change is shown in Fig. 15.

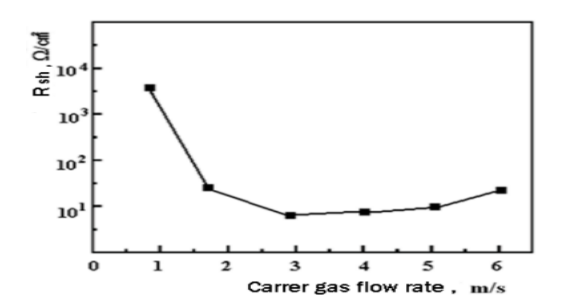


Fig. 8 Changes in membrane surface resistance with carrier gas flow rate

In Fig. 8, the film surface resistance decreased and then showed an increasing trend with increasing carrier gas flow rate. At a carrier gas flow rate of 1 m/s, the membrane surface resistance was very high, with a maximum value of 104  $\Omega/\text{cm}^2$ , gradually decreasing from 2 m/s to 8  $\Omega/\text{cm}^2$  at 3 m/s, and slightly increasing from the central part at 4 m/s to 5 m/s. Also, as the carrier gas flow rate increased, the nozzle shape was significantly different in the surface resistance characteristics due to the non-uniform film thickness at the center and edge of the substrate. The film was homogeneous when the carrier gas flow rate was less than 3 m/s, but the surface resistance was very high, and the difference was almost as severe as 10-50  $\Omega/\text{cm}^2$  when the carrier gas flow rate was higher than 3 m/s. When the carrier gas flow rate was 1 m/s, the transmittance of the film showed a maximum transmittance of 88% in the visible region, and 80% in the visible region at 3 m/s. The lowest transmission in the 350 nm wavelength range was found at a carrier gas flow rate of 5 m/s. At a constant jet distance, the carrier gas velocity of 1 m/s was such that the atomized fogs were pyrolyzed and nucleated and evaporated by heat convection, without overcoming the upward convective flow due to the substrate thermal energy and reaching the substrate. Hence, the film formation rate and efficiency were low, and only the grains with large grains were attached to the substrate, which increased the transmittance and surface resistance properties. On the other hand, when the carrier gas flow rate was around 5 m/s, the spray particle collided with the substrate at a high rate and increased the nucleus and crystal growth attached to the substrate for a unit time, resulting in an increase in particle size, thereby decreasing the film transmittance and surface resistance in the visible region.

#### Effect of distance between substrate and spray nozzle

To study the effect of the distance between the substrate and the spray nozzle, the distance between the nozzle and the substrate was varied from 0.5 to 1.1 cm, and the pyrolysis temperature was set at 500 °C, carrier gas flow rate of 3 m/s and deposition time was set at 15 min using the precursor solution described previously. Based on these process parameters, the morphology, light transmittance and surface resistance of the fabricated FTO films were measured. Fig. 9 shows the variation of transmittance and surface resistance with the distance between the substrate and the spray nozzle.

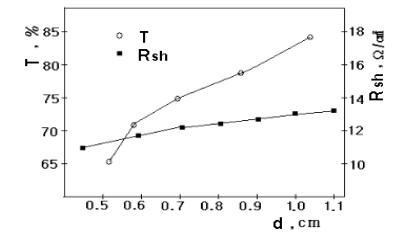


Fig. 9 Transmittance and surface resistance variation with the distance between substrate and spray nozzle.



In the figure, as the distance between the spray nozzle and substrate increased, the transmittance changed linearly with the slope greatly, and the surface resistance changed smoothly. The lower nozzle substrate distance increased the heat loss of the substrate by spraying the adherent substrate. This is likely due to the growth of the crystalline particles that have not been fully pyrolyzed on the substrate, which does not allow for rapid replenishment of the lost heat. Also, if the distance between the substrate glass heated at high temperature and the spray nozzle was too close, the substrate was damaged due to thermal shock of the substrate. It can be seen that the distance between the spray nozzle and the substrate with excellent electro-optic properties is between 0.5 and 0.9 cm.

Changes in the electrooptical properties of FTO films with the concentration of spray solution

Fig. 10 shows the surface resistivity and transmittance profiles of FTO films with respect to the stannous chloride concentration. As can be seen in Fig. 10, the surface resistance of the transparent conductive film gradually decreases with increasing the concentration of tin chloride. From the graph in Fig. 10, the relationship between the concentration of tin chloride (N) and the surface resistance is expressed as Eq. 1.

Rsh= 
$$5.3275N - 0.803$$
 (2)

 $L^2 = 0.9453$ 

Here L is the squared error between the functional expression and the measured value.

Through this square error value, the functional expression can be approximated to correspond to the relationship between surface resistance and stannous chloride concentration.

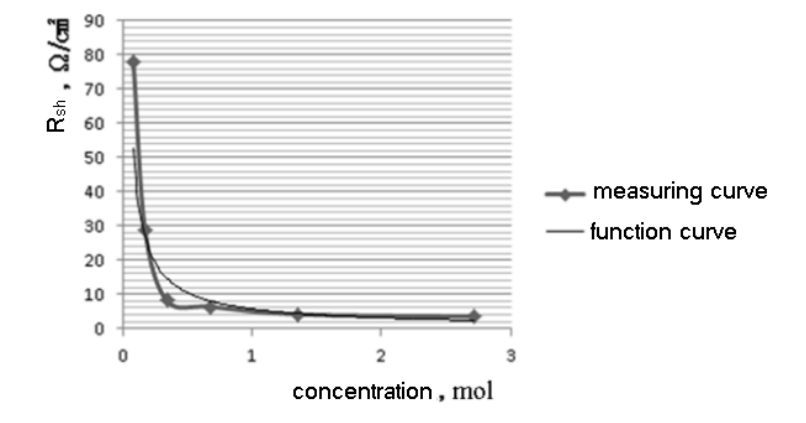


Fig. 10 Surface resistance of FTO films with stannous chloride concentration

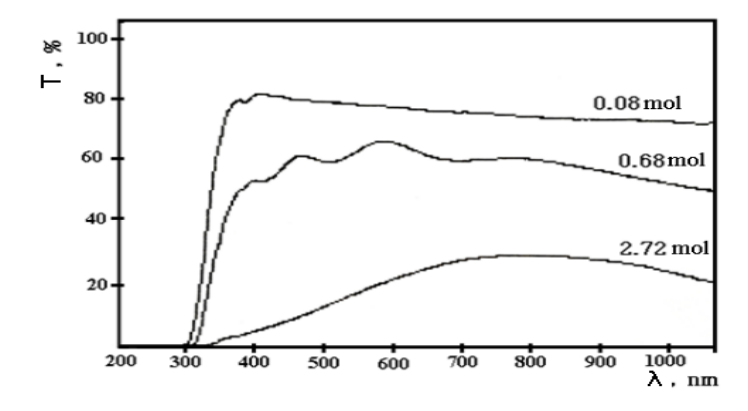


Fig. 11 Transmittance profiles of FTO films with stannous chloride concentration

As the concentration of tin chloride increases, the lattice defects increase due to the substitution of Cl atoms in the SnO2 lattice. The decrease in surface resistance and transmittance is due to the increase in crystallinity of the films.





#### **Effect of fluorine impurity**

Table 1 shows the change in surface resistance with stannous chloride concentration and doping amount and average transmittance variation in the range of 300-800 nm.

Table 2. Variation of properties with stannous chloride concentration and doping

SnCl <sub>4</sub> ,	Impurity Concentration,0.027 mol		Impurity concentration, 0.054mol		Impurity concentration, 0.08mol		Impurity concentration, 0.1mol		Impurity concentration, 0.135mol	
	$R_{sh}$ , $\Omega$ /cm²	T, %	$R_{\mathrm{sh}}$ , $\Omega$ /cm²	T, %	$R_{sh}$ , $\Omega$ /cm²	T, %	$R_{sh}$ , $\Omega$ /cm²	T, %	$R_{sh},\Omega$ /cm²	T, %
1.08	200	85	105	82	78	83	65	80	45	79
1.17	100	83	75	81	29	81	20	78	18	75
1.34	56	82	35.4	80	10.2	78	6.8	76	5.6	71
1.68	35	80	28.6	79	6.4	76	5.5	63	3.5	60
2.36	20	77	12.2	68	4.2	65	3.2	62	2.6	59
3.72	12	69	7.5	56	3.5	51	2.8	48	2	45

Table 2 shows low surface resistance to less than  $10~\Omega$  /cm when the concentration of ammonium fluoride is higher than 1.34 mol and the concentration of ammonium chloride is higher than 1.08 mol. This is due to the increased charge carriers in the film crystals.

However, as the concentration of tin chloride and dopant increased, the average transmittance of the 300-800 nm wavelength decreased by 45%. The surface resistivity decreased with increasing concentration and doping of stannous chloride and changed almost uniformly from 1.08 mol to more. The reason is that the amount of fluorine atoms substituted with oxygen atoms in SnO2 crystals increases, acts as impurities and increases the carrier scattering phenomenon, which leads to a decrease in charge carrier concentration and a larger crystallite size [40, 41].

Also, the reason for the rapid decrease in average transmittance at 300-800 nm with the concentration of tin chloride and dopant is thought to be due to the increase in the size of the crystal particles, which leads to the increase in the film thickness, which leads to the transmission of light in this wavelength range, and thus to the reflection or scattering [42].

#### CONCLUSIONS

A spray nozzle was designed to prepare FTO thin films by ultrasonic spray pyrolysis process, the carrier gas flow characteristics were simulated, and the film uniformity was evaluated by surface resistance. The process conditions for the preparation of the films used in the experiments were: SnCl4 concentration of 1.34 mol, NH4F concentration of 0.08 mol, temperature of 500°C, deposition time of 15 min, carrier gas flow rate of 3m/s, distance between nozzle and substrate of 0.7 cm. The transmittance of the fabricated FTO film was around 80%. The prepared FTO films showed a uniform behavior with surface resistance between 14 and  $15\Omega$ /cmand X-ray analysis showed a high orientation of SnO2 crystals in the 200-plane. SEM analysis showed that the crystallite size was constant.

Further investigation of the process in more detail is required to improve the transmittance and surface resistance of FTO films based on the simulation of the homogeneous characteristics of the heating process.

ISSN No. 2454-6194 | DOI: 10.51584/IJRIAS | Volume X Issue IX September 2025



#### REFERENCES

- 1. S. Calnan, A.N. Tiwari. High mobility transparent conducting oxides for thin film solar cells. Thin Solid Films 518 (2010), 1839.
- 2. G. Granqvist, Transparent conductors as solar energy materials: a panoramic review, Sol. Energy Mater. Sol. Cells 91, 1529–1598 (2007).
- 3. S. Aukkaravittayapun, N. Wongtida, T. Kasecwatin, Large scale F-doped SnO2 coating on glass by spray pyrolysis, National Metal and Materials Technology Center, 1-4(2005)
- 4. C.R. Osterwald, T.J. McMahon, J.A. del Cueto, Electrochemical corrosion of SnO2: F transparent conducting layers in thin film photovoltaic modules, Sol. Energy Mater. Sol. Cells 79 (2003) 21–33.
- 5. S. Sujatha Lekshmy, G.P. Daniel, K. Joy, Microstructure and physical properties of sol gel derived SnO2: Sb thin films for optoelectronic applications, Appl. Surf. Sci. 274 (2013) 95–100.
- 6. Ch.M. Wang, Ch.C. Huang, J.Ch. Kuo, J.L. Huang, Investigation of pulsed ultraviolet laser annealing of Sb/SnO2 thin films on the structural, optical and electrical properties, Surf. Coat. Technol. 231 (2013) 374–379.
- 7. B Benhaoua, S Abbas, A Rahal, A Benhaoua, M.S. Aida, Effect of film thickness on the structural, optical and electrical properties of SnO2: F thin films prepared by spray ultrasonic for solar cells applications. Superlattices and Microstructures 83 (2015) 78–88
- 8. H. Köse, A.O. Aydin, H. Akbulut, Sol–gel synthesis of nanostructured SnO2 thin film anodes for Liion batteries, Acta Phys. Pol. A 121 (2012) 227–229.
- 9. R.H.R. Castro, J. Pereira Gilberto, Douglas Gouvea, Surface Modification of SnO2 Nanoparticles Containing Mg or Fe: Effects on Sintering, Appl. Surf. Sci. 253 (2007) 4581.
- 10. G. Korotcenkov, I. Boris, V. Brinzari, S.H. Han, B.K. Cho, The role of doping effect on the response of SnO2-based thin film gas sensors: analysis based on the results obtained for Co-doped SnO2 films deposited by spray pyrolysis, Sens Actuat B 182 (2013) 112–124.
- 11. E. Zampiceni, E. Bontempi, G. Sberveglieri, L.E. Depero, Mo influence on SnO2 thin films properties, Thin Solid Films 418 (2002) 16–20
- 12. G. Turgut, Investigation of characteristic properties of Pr-doped SnO2 thin films, Philosophical Magazine, 95 (2015) 1607–1625.
- 13. G. Turgut, E.F. Keskenler, S. Aydın, E. Sönmez, S. Dogan, B. Düzgün, M. Ertugrul, Effect of Nb doping on structural, electrical and optical properties of spray deposited SnO2 thin films, Superlattices Microstruct. 56 (2013) 107–116.
- 14. R. Thomas, T. Mathavan, Mohd. Shkir, Opto-electronic properties of Ce-doped FTO thin films prepared using Nebulizer spray technique for TCO application Optik (2020) 1-31
- 15. F Gao, G Qin, Y Li, Q Jiang, Li Luo, K Zhao, Y Liu, One-pot synthesis of La doped SnO2 layered nanoarrays with enhanced gas-sensing performance toward acetone, RSC Advances, DOI: 10.1039/C5RA27270J.
- 16. B.H. Liao, C.C. Kuo, P.J. Chen, and C.C. Lee, Fluorine doped tin oxide films grown by pulsed direct current magnetron sputtering with an Sn target, Appl. Opt. 50, C106–C110 (2011).
- 17. B H Liao, S H Chan, C C Lee, FTO films deposited in transition and oxide modes by magnetron sputtering using tin metal target Appl. Opt. 53(4), (2011), A148–A153
- 18. H. Köse, A.O. Aydin, H. Akbulut, Sol–gel synthesis of nanostructured SnO2 thin film anodes for Liion batteries, Acta Phys. Pol. A 121 (2012) 227–229.,
- 19. B. Zhu, Ch. Yin, Z. Zhang, Ch. Tao, Liu Yang, Investigation of the hydrogen response characteristics for sol–gel-derived Pddoped, Fe-doped and PEG-added SnO2 nano-thin films, Sens Actuat B 178 (2013) 418–425.
- 20. K. Murakami, K. Nakajima, S. Kaneko, Initial growth of SnO2 thin film on the glass substrate deposited by the spray pyrolysis technique, Thin Solid Films 515 (2007) 8632–8636.,
- 21. S.M. Sabnis, A. Prakash, Bhadane, P.G. Kulkarni, Process flow of spray pyrolysis technique, IOSR Journal of Applied Physics 4, (2013), 2278-4861.
- 22. A Kashinath Bogle, D. Kiran More, Sumayya Begum, W. Jagdish Dadge, P. Megha Mahabole, S. Rajendra Khairnar, Optical and electrical properties of F doped SnO2 thin films, Indian Journal of Pure & Applied Physics 56 (2018) 755-758.

ISSN No. 2454-6194 | DOI: 10.51584/IJRIAS | Volume X Issue IX September 2025



- 23. A. Adjimi, M.S Aida, N Attaf, Y.S Ocak, Gadolinium doping effect on SnO2 thin films optical and electrical properties, Mater. Res. Express 6 (2019) 096405
- 24. Y. Ziad Banyamin, J. Peter Kelly, Glen West, Jeffery Boardman, Electrical and Optical Properties of Fluorine Doped Tin Oxide Thin Films Prepared by Magnetron Sputtering, Coatings 4 (2014) 732-746.
- 25. A.A. Yadav, E.U. Masumdar, A.V. Moholkar, M. Neumann-Spallart, K.Y. Rajpure, C.H. Bhosale, Electrical, structural and optical properties of SnO2:F thin films: Effect of the substrate temperature, Journal of Alloys and Compounds 488 (2009) 350–355.
- 26. K. Deva Arun Kumar, S. Valanarasu, K. Jeyadheepan, Hyun-Seok Kim, Dhanasekaran Vikraman, Evaluation of the physical, optical, and electrical properties of SnO2: F thin films prepared by nebulized spray pyrolysis for optoelectronics, Journal of Materials Science: Materials in Electronics 29 (2018) 3648–3656.
- 27. E. Elangovan, M.P. Singh, K. Ramamurthi, Studies on structural and electrical properties of spray deposited SnO2: F thin films as a function of film thickness, Materials Science and Engineering B 113 (2004) 143–148.
- 28. A.V. Moholkar, S.M. Pawar, K.Y. Rajpure, C.H. Bhosale, J.H. Kim, Appl. Surf. Sci. 255 (2009) 9358–9364.
- 29. Q.N. Zhao, S. Wu, D.K. Miao, Adv. Mater. Res. 150-151 (2011) 1043-1048.
- 30. E.V.A. Premalal, N. Dematage, S. Kanko, A. Konno, Electrochemical 80 (2012) 624–628.
- 31. D.S. Bhachu, M.R. Waugh, K. Zeissler, W.R. Branford, I.P. Parkin, Chem. Eur. J. 17 (2011) 11613–11621.
- 32. H.L. Zhao, Q.L. Liu, Y.X. Cai, F.C. Zhang, Mater. Lett. 62 (2008) 1294–1296.
- 33. J.K. Yang, W.C. Liu, L.Z. Dong, Y.X. Li, C. Li, H.L. Zhao, Appl. Surf. Sci. 257 (2011) 10499–10502.
- 34. A. Graaf, J.V. Deelen, P. Poodt, T. Mol, K. Spee, F. Grob, A. Kuypers, Energy Procedia 2 (2010) 41–48.
- 35. H. Kim, R.C.Y. Auyeung, A. Piqué, Thin Solid Films 520 (2011) 497–500
- 36. A. Benhaoua, A. Rahal, B. Benhaoua, M. Jlassi, Effect of fluorine doping on the structural, optical and electrical properties of SnO2 thin films prepared by spray ultrasonic, Superlattices Microstruct. 70 (2014) 61–69.
- 37. A. Rahal, S. Benramache, B. Benhaoua, Preparation of n-type semiconductor SnO2 thin films, J. Semiconduct. 34 (8) (2013) 1–4.
- 38. Z.B. Zhou et al; Preparation of indium tin oxidefilms and doped tin oxide films by an ultrasonic spray CVD process, Applied Surface Science, 172, (2001), 245-252.
- 39. B Suer, M Ozenbas, Conducting fluorine doped tin dioxide(FTO) coatings by ultrasonic spraysis for heating applications, Ceramics International, vol47, (2021), 17242-17254
- 40. Sahrul Saehana, Aqidatul Izzah, et al, Fabrication of Fluorine-Doped Tin Oxide (FTO): From experiment to its application in physics learning, 7(2), (2023), 259-268
- 41. N Guermat, er al, Super-Hydrophobic F-Doped SnO2 (FTO) Nanoflowers Deposited by Spray Pyrolysis Process for Solar Cell Applications. Journal of Nano- and Electronic Physics, 14(5), (2022), 05013-1–05013-6.
- 42. R R-Amador, J J Alvarado-Pulido, Study of fluorine-doped tin oxide thin films deposited by pneumatic spray pyrolysis and ultrasonic spray pyrolysis: a direct comparison, Mater. Res. Express, 10, (2023), 066402